HHS Public Access

Author manuscript

Technol Cancer Res Treat. Author manuscript; available in PMC 2015 April 26.

Published in final edited form as:

Technol Cancer Res Treat. 2015 April ; 14(2): 213–220. doi:10.7785/tcrt.2012.500400.

Small Portable Interchangeable Imager of Fluorescence for Fluorescence Guided Surgery and Research

Olugbenga T. Okusanya, M.D.[1,*], **Brian Madajewski, B.A**[1], **Erin Segal**[1], **Brendan F. Judy, B.A**[1], **Ollin G. Venegas, B.A**[1], **Ryan P. Judy, B.A**[1], **Jon G. Quatromoni, B.A**[1], **May D. Wang, Ph.D**[2], **Shuming Nie, Ph.D**[3], and **Sunil Singhal, M.D**[1]

[1]Thoracic Surgery Research Laboratory, Department of Surgery, University of Pennsylvania, Perelman School of Medicine, Philadelphia, PA

[2]Department of Biomedical Engineering, Georgia Institute of Technology, Atlanta, Georgia

[3]Departments of Biomedical Engineering and Chemistry, Emory University, Atlanta, Georgia

Abstract

Fluorescence guided surgery (FGS) is a developing field of surgical and oncologic research. Practically, FGS has shown useful applications in urologic surgery, benign biliary surgery, colorectal cancer liver metastasis resection, and ovarian cancer debulking. Most notably in in cancer surgery, FGS allows for the clear delineation of cancerous tissue from benign tissue. FGS requires the utilization of a fluorescent contrast agent and an intraoperative fluorescence imaging device (IFID). Currently available IFIDs are expensive, unable to work with multiple fluorophores, and can be cumbersome. This study aims to describe the development and utility of a small, cost-efficient, and interchangeable IFID made from commercially available components. Extensive research was done to design and construct a light-weight, portable, and cost-effective IFID. We researched the capabilities, size, and cost of several camera types and eventually decided on a near-infrared (NIR) charged couple device (CCD) camera for its overall profile. The small portable interchangeable imager of fluorescence (SPIIF) is a “scout” IFID system for FGS. The main components of the SPIIF are a NIR CCD camera with an articulating light filter. These components and a LED light source with an attached heat sink are mounted on a small metal platform. The system is connected to a laptop by a USB 2.0 cable. Pixielink © software on the laptop runs the system by controlling exposure time, gain, and image capture. After developing the system, we evaluated its utility as an IFID. The system weighs less than two pounds and can cover a large area. Due to its small size, it is easily made sterile by covering it with any sterile plastic sheet. To determine the system’s ability to detect fluorescent signal, we used the SPIIF to detect indocyanine green under *ex* and *in-vivo* conditions and fluorescein under *ex-vivo* conditions. We found the SPIIF was able to detect both ICG and fluorescein under different depths of a semi-opaque colloid. Second, we found that a concentration as low as 0.5 g/ml of indocyanine green dissolved in plasma was detectable. Lastly, in a murine and human cancer model, the SPIIF was

*Corresponding author: Olugbenga T. Okusanya, M.D., Phone: 2155198170, Olugbenga.Okusanya@uphs.upenn.edu.

Conflict of Interest

All authors certify that his manuscript has not been published in whole or in part nor is it being considered for publication elsewhere. The authors have no conflicts of interest to declare.

able to detect indocyanine green signal within tumors and generate a signal-to-background ratio (SBR) of 3.75. This study shows that a low-cost IFID can be made from commercially available parts. Second, this IFID is capable of *in* and *ex-vivo* detection of multiple fluorophores without sacrificing its small size or favorable ergonomics.

Keywords

Intraoperative imaging; Fluorescence guided surgery; Indocyanine green; Near infrared

Introduction

In the last 10 years, surgeons have become interested in fluorescence guided surgery (FGS) (1–4). FGS is a technique by which a fluorophore is systemically injected into a patient or locally injected into the tissue of interest and fluorescent imaging is performed in real-time to aid the surgeon. FGS has shown practical applications for oncologic resections, general surgery, gynecologic, and neurosurgical procedures (5–9). Specifically, FGS has allowed surgeons to detect sentinel lymph nodes, identify complicated biliary anatomy, and detect sites of metastatic disease. FGS depends on fluorescent contrast agents (targeted and non-specific) and intraoperative fluorescence imaging devices (IFID). Though only a few FDA approved contrast agents exist, many clinical-grade IFIDs are available.

Most of the clinical-grade IFIDs are hampered by their high cost, limited portability, and lack of flexibility. The size and cost of these systems are a result of the multiple high quality cameras, light sources, and computing systems that are used to construct them. Some of the currently available systems weigh 270 pounds and cost upwards of $275,000. Another drawback to these systems is that they are configured to work only with NIR contrast agents and many cannot be adapted to work with tracers of different wavelengths (10, 11). Altering these systems to work with a range of contrast agents would essentially require deconstructing them to change internally located light filters on both the camera system and fluorescent light sources. There are already at least two FDA approved contrast agents (indocyanine green and fluorescein) which have different fluorescent properties. Numerous other contrast agents with even more variable fluorescent properties are currently being used in research and many are in the process of gaining FDA approval. The limitations of these commercially available systems leave a niche to be filled in the field of FGS research.

The ideal IFID should have several properties for FGS. First, it should be able to excite and detect the signal from a given fluorophore on a macroscopic scale. It should contain a light source and a filter system that excites the fluorophore and detects the omitted signal. Second, a preferred IFID would be able to work with a range of tracers with different excitation and emissions spectra. Third, it should be operating room-friendly, *i.e.*, portable, adjustable, and amenable to sterilization. Fourth, interpretation of data from the system should be straight-forward. Areas with fluorescent signal must be clearly demarcated from other areas. Lastly, the system should be reasonably priced.

We have developed a portable, modular IFID for FGS for less than $3,200. This system, named the Small Portable Interchangeable Imager of Fluorescence (SPIIF), satisfies the

guidelines for an ideal IFID. At its rudiments, the SPIIF consists of a near-infrared charged couple device (CCD) camera mounted with an adjustable filter holder and a LED light source on one platform. The data from the SPIIF is displayed on screen in real-time and is compiled using Image J ©, a free, publicly available image processing software. The SPIIF weighs less than 3 pounds and is easy to use in both the clinical and laboratory setting. Here, we demonstrate that this system works with fluorescein and ICG, but it also has the theoretical ability to work with a range of other fluorophores without difficulty or excessive cost.

Materials and Methods

Camera

A CCD camera was chosen as an image capture device for the combination of size, quality, price, and availability. A 1.3 MP USB 2.0 Monochrome CCD camera (Catalog #PL-B741EU, Edmund Optics, Barrington, NJ) was attached to a metal platform using four screws. The camera has a maximum resolution of 1280 × 1024 pixels and records at a maximum of rate of 24 frames per second. A monochromatic camera was chosen to simplify the color display and to maximize fluorescent signal.

Mechanical System

A 6.5 inch by 4.5 inch by ¼ inch steel-mounting platform was custom built by BioMedicon © (Moorestown NJ). Four screws and a washer system were used to mount the CCD camera and the LED light source to the platform. An articulating arm with a light filter holder was also mounted to the platform. A modular anchoring system that fit either a clamp or 5-inch plastic handle was attached to the underside of the metal platform (Figure 1).

A piece of one inch thick black phenolic sheet was fashioned as a background for mounted experiments. This material and color were chosen to minimize background signal and glare.

Light Perception and Optics

A 16 mm VIS Compact Fixed Focal Length lens was attached to the CCD camera. This lens allows for a minimum working distance of 10 cm and allows for easy hand-held image focusing. Mounted in front of the lens is the light filtration system. A lens filter holder (THORlabs, Newton NJ Catalog #TRF90) was mounted directly to the steel platform with the rotating arm for the filter placing it directly in front of the lens. Within the holder, the fluorescence bandpass filter is held in place by a washer and c-mount thread system. This filter can be changed to the appropriate emission spectra of the dye in use (Figure 2).

Light Excitation

A SY LED spot light of 740 nm (Edmunds Optics, Catalog #NT63-338) or a SY LED spot light of 395 nm (Edmunds Optics, Catalog #NT63-335) were mounted directly onto a SY LED Area Light Heat Sing (Edmunds Optics, Catalog #NT63-342). The 740 nm LED was used for indocyanine green and the 395 nm LED was used for fluorescein. This construct was then anchored to the steel platform using a screw and washer mechanism. This allows

the light to be targeted to a specific area at a specific angle while keeping the system confined to a single mounting.

Computer & Software

The captured image from the CCD camera was transmitted via USB 2.0 to a Hewlett Packard Probook 4520 laptop running Windows 7. PixeLINK Capture OEM, is an image acquiring software that runs the camera and also controls image acquisition. Many variables could be adjusted using PixeLINK, including frame rate, saturation, brightness, and exposure time. PixeLINK images were also viewed in a high-resolution preview mode to observe changes in real-time. Black and white images were further processed using Image J to superimpose a green tint.

In Vitro Model

Depth of signal detection and minimum detectable concentration were interrogated using *in vitro* models. First, 125 μL of a 2.5×10^{-3} mg/ml concentration of ICG in plasma and 125 μL of a 18.4 uM concentration of an FDA folate-FITC conjugate dissolved in normal saline were placed at the bottom of a plastic container. A semi-opaque solution, liquefied butter, was layered in these containers to a depth of 0 cm, 0.5 cm, 1 cm and 1.5 cm. Subjective fluorescence was determined by investigators while Region of Interest (ROI) software (within Image J) was used to determine a signal-to-background ratio (SBR) at each depth.

To determine the limit of detection of the SPIIF, 2 mg of ICG was dissolved in 1 ml of plasma and serially diluted 12 times to a final ratio of 1:20,000. One hundred microliters of stock solution and each dilution was then placed in consecutive wells in a black 96 well plate. Plates were then imaged using the SPIIF at a distance of 18 cm. The images were processed in Image J. ROI software was used to generate SBRs.

Animal Experimental Model

Twenty female C57BL/6 mice were purchased from Charles River Laboratories and Jackson Laboratories. All mice were maintained in pathogen-free conditions and used for experiments at ages eight weeks or older. The Animal Care and Use Committees of the Children's Hospital of Philadelphia, The Wistar Institute, and the University of Pennsylvania approved all protocols in compliance with the Guide for the Care and Use of Laboratory Animals. The metastatic murine non-small-cell carcinoma (NSCLC) cell line and the murine Lewis Lung Carcinoma (LLC) cell line were obtained from American Type Culture Collection (Manassas, VA) and cultured in high-glucose DMEM (Dulbecco's Modified Eagle's Medium, Mediatech, Washington, DC) supplemented with 10% fetal bovine serum (FBS; Georgia Biotechnology, Atlanta, GA), 1% penicillin/streptomycin, and 1% glutamine. Cell lines were regularly tested and maintained negative for *Mycoplasma spp.*

Twenty mice were injected with 2×10^6 LLC cells in their right flanks. After two weeks of growth, each mouse was injected with ICG via tail vein, as previously described and then imaged with the SPIIF (12).

Human Experimental Model

As a part of a pilot clinical trial, a 45 year old man with a known history of a thoracic osteosarcoma was given ICG to determine if the SPIIF could intraoperatively identify fluorescent signal from within the tumor. After the tumor was resected, it was imaged *ex vivo* using the SPIIF. Images were collected and processed with Image J and compared to final pathology. ROI measurements were taken over tumor and normal chest wall and a SBR was determined. All research was approved by the IRB at the University of Pennsylvania and the patient gave informed consent for the procedure.

Results

Accessibility

Currently, IFIDs can only be attained from a few companies and require a substantial financial investment. In order to show that an affordable and readily accessible IFID can be made, we sought to develop the SPIIF using cost-sensitive commercially available components. We researched commercially available camera types ranging from CCD, complementary metal oxide semiconductors (CMOS), and tube cameras. We then researched all other components based on their commercial availability, cost, and ability to work with visible and near infrared light.

We found cameras that met our criteria from Pixelink®, JAI®, Hamamatsu®, Princeton Instruments® and Basler®. We ultimately selected a NIR black and white CCD from Pixelink® due cost, size, and ability to work with NIR light. A black and white configuration was chosen for ease of data interpretation. With regard to the lens, we chose a 16 mm NIR lens for wavelength compatibility and ideal working distance for a hand held configuration. LED light sources were chosen in order to avoid potentially dangerous laser light sources, low cost, and long bulb life. Light filters and holders were ordered from Edmunds Optics and Chroma for cost savings. No component itself was altered after purchase. All mounting was performed by Biomedicon®, a local medical engineering firm, and could easily be replicated by any serviceable machine shop. In total, the system cost $3,200 (Table I).

We found that an IFID could be created from commercially available products without excessive cost and with limited aftermarket modifications.

Ergonomics

Some available IFIDs are large and cumbersome. In order to show that ergonomic IFIDs are attainable, we created the SPIIF from small low-weight components that could be constrained to a limited space. When designing the system, the simplest possible schema was chosen. When researching camera systems and component parts, the lightest and smallest components were selected. Any extra weight, unnecessary casing, or computing technologies were avoided.

First, we designed a system that only utilized one camera to avoid adding extra bulk. Second, a simple NIR CCD camera was chosen for its weight of less-than-a pound, which allowed the system to be operated by a laptop rather than a more cumbersome high-end

computing system (that would be needed to integrate multiple images). LED light sources, which do not require cooling fans or large power sources, were selected because of their ability to be contained to a small space and their ability to deliver sufficient light over a contained area. Of note, a 395 nm LED was chosen for fluorescein because the broad excitation spectra of these particular LED lights could cause interference with the emission spectra of fluorescein. A small, lightweight heat sink was more than sufficient to dissipate the heat generated from the LED. Lastly, the entire system was mounted to one 11 cm by 16 cm metal plate (Figure 1). The excitation filter and LED light source were mounted in such a way that they can both be easily changed without deconstructing the whole system. Thus, changing the SPIIF to work with different contrast agents is simple and straightforward. Additionally, the entire platform was constructed to allow either portable imaging using a small handle or stationary imaging using a C clamp. In total, the system weighs less than 2 pounds (Figure 2). With extended power and USB cables, the SPIIF can cover an area of 85.9 m^2. With its current size, the entire system can easily be made sterile by covering it with any number of sterile plastic operating room drapes.

The SPIIF is an ergonomic IFID created from small, lightweight parts, as opposed to the cumbersome nature of some commercially available IFIDs.

Detection Capacity

IFIDs must be able to reliably detect a range of contrast agents. To ascertain if the SPIIF would be able to detect multiple fluorescent contrast agents, we used the SPIIF to detect two contrast agents in varying conditions. Standard concentration and volumes of ICG and a folate-fluorescein conjugate were placed in variable depths of a semi opaque colloid (liquefied butter). Second, serial dilutions of ICG mixed with plasma were made and imaged with the SPIIF. ROI software was used to confirm subjective fluorescence in both settings.

The SPIIF was able to create a SBR of 17.3, 6.5, 2.4 & 1.5 at depths of 0, 0.5, 1, and 1.5 cm, respectively, for ICG and 38, 6.8, 1.4, and 1 for the folate-fluorescein conjugate at the same depths. We found that a SBR greater than 2 correlated to subjective fluorescence and the SPIIF was able to generate a SBR of greater than 2 at a depth of 1cm of colloid for ICG. For the folate FITC conjugate, the SPIIF generated a SBR greater than 2 at depths of 0 cm and 0.5 cm only. We also found that the SPIIF was readily able to detect between 0.5 μg/ml and 2 mg/ml of ICG in plasma (Figure 3).

The SPIIF shows the ability to detect multiple contrast agents under a range of conditions proving that its design enables it to work as a simple straightforward fluorescence detection device.

FGS Applications

IFIDs must be able to detect fluorescent signal in practical FGS situations. To prove that the SPIIF would be able to detect fluorescent signal in the *in vivo* setting, we used the SPIIF to detect signal from a preclinical and clinical FGS model.

Twenty mice with flank LLC tumors were injected with ICG, as previously described (12). The mice were subsequently imaged using the SPIIF. Of the twenty LLC mice injected with

ICG, twenty showed positive NIR signal with the spectrometer. All images obtained by the SPIIF showed a signal in the flank tumor and in the tail injection site (Figure 4). No mice showed false negative or false positive signals. The signal demonstrated a high degree of accuracy, as it remained confined to the tumor (peritumoral tissues showed no signal).

Next, one patient with a known osteosarcoma was injected with ICG and had his tumor imaged using the SPIIF post-resection. SBR values were generated using ROI software within Image J. ICG signal was clearly found in the tumor of the patient when imaged *ex-vivo*. Signal intensity was strong within the tumor and a peak SBR of 3.75 was found when the tumor specimen was opened and imaged (Figure 5). On final pathology, the areas that proved to be tumor corresponded with areas of fluorescence imaged with the SPIIF. The SPIIF here showed itself to be a useful and viable IFID.

Discussion

The SPIIF fills a current need for surgeons performing FGS research. While FGS is a growing field, it remains significantly hindered by the lack of accessible IFIDs. In the last year, more than thirty papers on surgical applications of FGS were published. However, the cost, size, range, and modularity of current available IFIDs limit investigators from participating in FGS research. The market for IFIDs still does not offer cheap hand-held systems that are attainable by most small to medium-sized laboratories. The SPIIF can serve as a ‘scout’ macroscopic system for FGS because of its accessibility, ergonomics, and utility. Admittedly, though systems like the Photodynamic Eye and the Artemis deliver higher quality images by utilizing spectral unmixing to enhance signal intensity and spacial resolution, they are not readily attainable by small or even medium-sized labs because of their prohibitive costs (13). Thus, the SPIIF and similar technologies occupy a unique role in this growing field.

The SPIIF has clear utility for FGS. The SPIIF was able to detect ICG and fluorescein while generating a significant SBR at comparable depths to other systems (14). The known depth of penetration of ICG signal has been shown to be less than 1 cm (15, 16). Our system was able to generate a SBR greater than 2 at this depth in a semi opaque colloid, thus showing sensitivity under these conditions. Not surprisingly, we could only generate a SBR great than 2 at 0.5 cm for fluorescein because of the visible light emission spectra of fluorescein. Our system was also able to detect small concentrations of ICG in plasma in the ex-vivo setting, suggesting more potential applicability in the clinical setting. Also, our limit of detection was 0.5 μg/ml (0.65 μM). This concentration is more than 100 times less than the peak fluorescence intensity of ICG in some *in-vivo* models (17). Second, our system’s limit of detection was lower than doses given in clinical trials (18, 19). Lastly, and most importantly, the SPIIF was able to detect NIR signal from tissues in both the laboratory and clinical setting, which proves to be its most valuable attribute. Clearly, these findings suggest that the SPIIF is a valid IFID for FGS.

There are several limitations to this system. First, the system is not able to display a real-time fluorescence and bright field overlay. However, the clear signal from the black and white camera display is sufficient to detect signal in real-time. Also, the hinged filter system

allows for rapid collection of both bright field and fluorescent images. Second, the system does not have an automated switching mechanism between filter sets. The filter and light source need to be manually changed. However, this adjustment is straightforward and can be performed in a few minutes. As others have discussed the idea of using a cocktail tracer approach may be the future of FGS which either have multiple filters in series or are able to rapidly switch filters (20). Other improvements to our system might involve coupling two very small CCD cameras together in order to generate an overlay. However, this will certainly add cost, some size, and complexity. Also, ideally, this system would also be completely wireless in order to further increase the range of the system and perhaps allow remote viewing by a surgeon or team experienced in FGS. Finally, it should be noted that our system is currently used for research purposes only. It cannot, and should not, be used for humans without institutional support.

Abbreviations

CCD	Charge Coupled Device
FGS	Fluorescence Guided Surgery
ICG	Indocyanine Green
IFID	Intraoperative Fluorescence Imaging Device
LLC	Lewis Lung Cancer
NIR	Near Infrared
ROI	Region of Interest
SBR	Signal to Background Ratio
SPIIF	Small Portable Interchangeable Imager of Fluorescence

References

1. Metildi CA, Kaushal S, Hardamon CR, Snyder CS, Pu M, Messer KS, Talamini MA, Hoffman RM, Bouvet M. Fluorescence-guided surgery allows for more complete resection of pancreatic cancer, resulting in longer disease-free survival compared with standard surgery in orthotopic mouse models. Journal of the American College of Surgeons 215. 2012:126–135. discussion 135–126. 10.1016/j.jamcollsurg.2012.02.021
2. Aydogan F, Ozben V, Aytac E, Yilmaz H, Cercel A, Celik V. Excision of nonpalpable breast cancer with indocyanine green fluorescence-guided occult lesion localization (IFOLL). Breast Care. 2012; 7:48–51.10.1159/000336497 [PubMed: 22553473]
3. Leon MB, Almagor Y, Bartorelli AL, Prevosti LG, Teirstein PS, Chang R, Miller DL, Smith PD, Bonner RF. Fluorescence-guided laser-assisted balloon angioplasty in patients with femoropopliteal occlusions. Circulation. 1990; 81:143–155. [PubMed: 2137043]
4. Tobis S, Knopf JK, Silvers CR, Marshall J, Cardin A, Wood RW, Reeder JE, Erturk E, Madeb R, Yao J, Singer EA, Rashid H, Wu G, Messing E, Golijanin D. Near infrared fluorescence imaging after intravenous indocyanine green: initial clinical experience with open partial nephrectomy for renal cortical tumors. Urology. 2012; 79:958–964.10.1016/j.urology.2011.10.016 [PubMed: 22336035]
5. Schols RM, Bouvy ND, van Dam RM, Masclee AA, Dejong CH, Stassen LP. Combined vascular and biliary fluorescence imaging in laparoscopic cholecystectomy. Surgical Endoscopy. 201310.1007/s00464-013-3100-7

6. Inoue S, Shiina H, Mitsui Y, Yasumoto H, Matsubara A, Igawa M. Identification of lymphatic pathway involved in the spread of bladder cancer: Evidence obtained from fluorescence navigation with intraoperatively injected indocyanine green. Canadian Urological Association Journal = Journal de l'Association des urologues du Canada. 2012:1–7.10.5489/cuaj.12096
7. Rossi EC, Ivanova A, Boggess JF. Robotically assisted fluorescence-guided lymph node mapping with ICG for gynecologic malignancies: a feasibility study. Gynecologic Oncology. 2012; 124:78–82.10.1016/j.ygyno.2011.09.025 [PubMed: 21996262]
8. Valdes PA, Bekelis K, Harris BT, Wilson BC, Leblond F, Kim A, Simmons NE, Erkmen K, Paulsen KD, Roberts DW. 5-Aminolevulinic-Acid-induced protoporphyrin IX fluorescence in meningioma: qualitative and quantitative measurements in vivo. Neurosurgery. 201310.1227/NEU.0000000000000117
9. van der Vorst JR, Schaafsma BE, Hutteman M, Verbeek FP, Liefers GJ, Hartgrink HH, Smit VT, Lowik CW, van de Velde CJ, Frangioni JV, Vahrmeijer AL. Near-infrared fluorescence-guided resection of colorectal liver metastases. Cancer. 201310.1002/cncr.28203
10. Vogt PR, Bauer EP, Graves K. Novadaq Spy Intraoperative imaging system--current status. The Thoracic and Cardiovascular Surgeon. 2003; 51:49–51.10.1055/s-2003-37276 [PubMed: 12587091]
11. Hutteman M, Mieog JS, van der Vorst JR, Liefers GJ, Putter H, Lowik CW, Frangioni JV, van de Velde CJ, Vahrmeijer AL. Randomized, double-blind comparison of indocyanine green with or without albumin premixing for near-infrared fluorescence imaging of sentinel lymph nodes in breast cancer patients. Breast Cancer Research and Treatment. 2011; 127:163–170.10.1007/s10549-011-1419-0 [PubMed: 21360075]
12. Madajewski B, Judy BF, Mouchli A, Kapoor V, Holt D, Wang MD, Nie S, Singhal S. Intraoperative near-infrared imaging of surgical wounds after tumor resections can detect residual disease. Clinical Cancer Research: An Official Journal of the American Association for Cancer Research. 2012; 18:5741–5751.10.1158/1078-0432.CCR-12-1188 [PubMed: 22932668]
13. Keereweer S, Kerrebijn JD, van Driel PB, Xie B, Kaijzel EL, Snoeks TJ, Que I, Hutteman M, van der Vorst JR, Mieog JS, Vahrmeijer AL, van de Velde CJ, Baatenburg de Jong RJ, Lowik CW. Optical image-guided surgery–where do we stand? Molecular Imaging and Biology: MIB: The official Publication of the Academy of Molecular Imaging. 2011; 13:199–207.10.1007/s11307-010-0373-2 [PubMed: 20617389]
14. De Grand AM, Lomnes SJ, Lee DS, Pietrzykowski M, Ohnishi S, Morgan TG, Gogbashian A, Laurence RG, Frangioni JV. Tissue-like phantoms for near-infrared fluorescence imaging system assessment and the training of surgeons. Journal of Biomedical Optics. 2006; 11:014007.10.1117/1.2170579 [PubMed: 16526884]
15. Jin H, Kang KA. Fluorescence-mediated detection of a heterogeneity in a highly scattering media. Advances in Experimental Medicine and Biology. 2005; 566:167–172.10.1007/0-387-26206-7_23 [PubMed: 16594149]
16. Solomon M, White BR, Nothdruft RE, Akers W, Sudlow G, Eggebrecht AT, Achilefu S, Culver JP. Video-rate fluorescence diffuse optical tomography for in vivo sentinel lymph node imaging. Biomedical Optics Express. 2011; 2:3267–3277.10.1364/BOE.2.003267 [PubMed: 22162817]
17. Mordon S, Devoisselle JM, Soulie-Begu S, Desmettre T. Indocyanine green: physicochemical factors affecting its fluorescence in vivo. Microvascular Research. 1998; 55:146–152.10.1006/mvre.1998.2068 [PubMed: 9521889]
18. Ishikawa K, Sasaki S, Furukawa H, Nagao M, Iwasaki D, Saito N, Yamamoto Y. Preliminary experience with intraoperative near-infrared fluorescence imaging in percutaneous sclerotherapy of soft-tissue venous malformations. Dermatologic Surgery: Official Publication for American Society for Dermatologic Surgery [et al.]. 2013; 39:907–912.10.1111/dsu.12152
19. Aldrich MB, Davies-Venn C, Angermiller B, Robinson H, Chan W, Kwon S, Sevick-Muraca EM. Concentration of indocyanine green does not significantly influence lymphatic function as assessed by near-infrared imaging. Lymphatic Research and Biology. 2012; 10:20–24.10.1089/lrb.2011.0003 [PubMed: 22416911]
20. Vahrmeijer AL, Hutteman M, van der Vorst JR, van de Velde CJ, Frangioni JV. Image-guided cancer surgery using near-infrared fluorescence. Nature Reviews. Clinical Oncology. 201310.1038/nrclinonc.2013.123

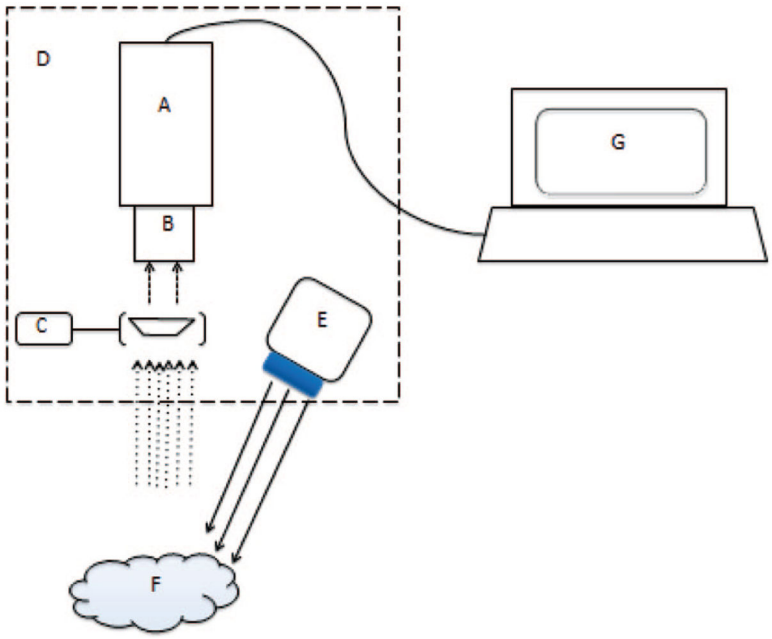

Figure 1.

Schematic representation of SPIIF. Components include (**A**) CCD Camera (**B**) NIR lens (**C**) Filter holder with filter (**D**) Metal plate (**E**) LED light source (**F**) Tumor (**G**) Laptop. This setup allows for all necessary components to be contained to one portable construct and only be tethered by a power cord and USB cable.

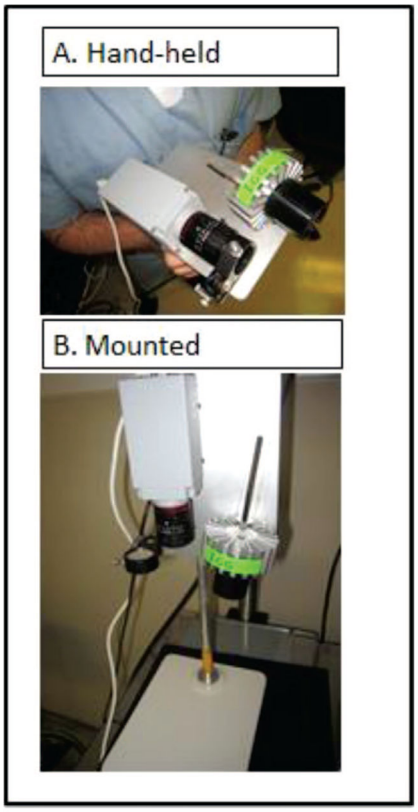

Figure 2.

Operational states of SPIIF. (**A**) SPIIF in its hand held configuration for *in vivo* use. It can easily be draped with sterile plastic if necessary. (**B**) SPIIF mounted on a standard lab mount for imaging *ex-vivo* specimens.

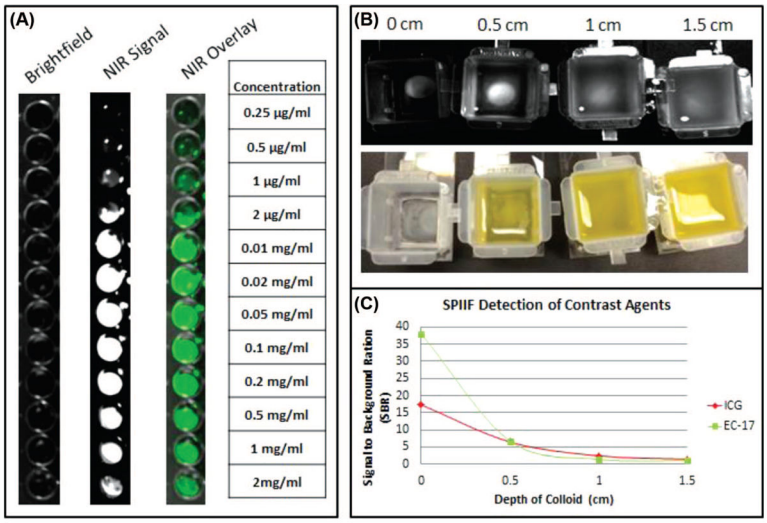

Figure 3.

ICG and Fluorescein Detection capacity of the SPIIF. (**A**) Standard black 96-well plate with various ICG concentrations in plasma. (**B**) ICG standard at various depths of a semi-opaque solution (liquefied butter). (**C**) Graph showing the SBR of ICG and fluorescein signal detected by the SPIIF and various depths.

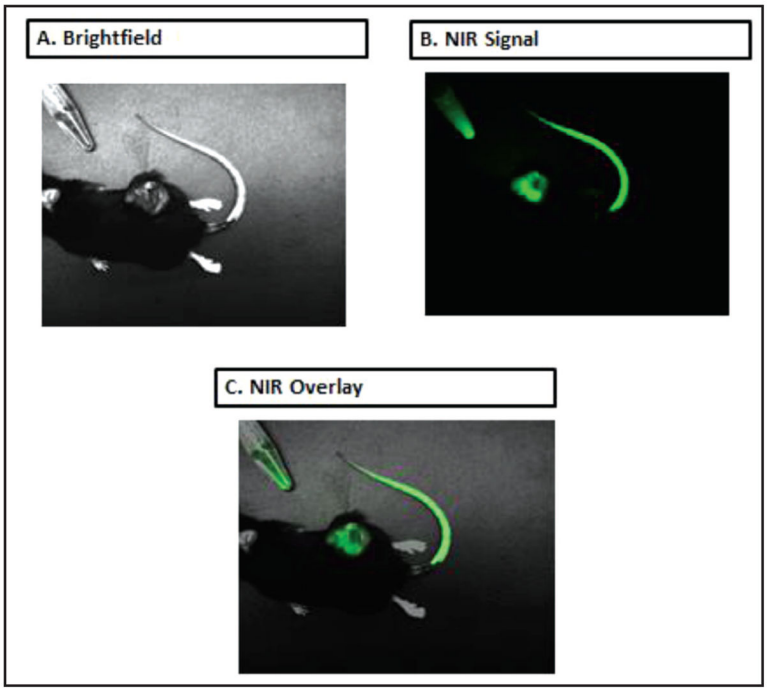

Figure 4.

SPIIF in laboratory use. SPIIF images from a LLC tumor bearing mouse model. (**A**) Brightfield (**B**) NIR fluorescence image from ICG within the tumor and tail vein injection site (**C**) Overlay.

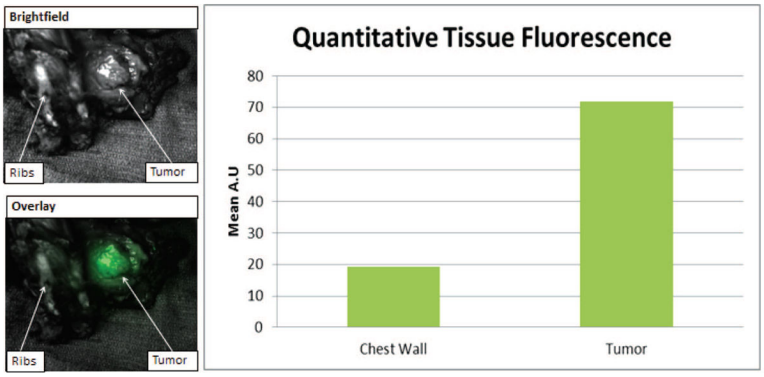

Figure 5.

SPIIF in clinical use. SPIIF images from a chest wall resection from a patient given a systemic dose of ICG. Bar graph shows quantitative fluorescence data from tumor and normal tissue.

Table I

List of SPIIF components with prices and various specifications.

Prototype system specs	
Camera	
Weight	0.46 lbs
Cost	$1,595
Computer interface	USB 2.0
Power source	USB
Shutter	100 s to 10 s
Frame rate	10
Lens	
Price	495
Focal length	16 mm
Mount	C-Mount
NIR Transmission	to 1000 nm
Light source	
Cost	~$550
Spot size	10 mm
Power source	AC input
Heat sink	
Cost	$50
Power source	
Cost	$295
Metal plate	
Size	16 × 11 × 0.5
Filter holder	
Cost	$78
Max filter size	9 mm
Total weight	2.0 lbs
Total price	$3,200